Simultaneous and independent multi-parameter monitoring with fault localization for DSP-based coherent communication systems

Thomas Shun Rong Shen,[1,*] Alan Pak Tao Lau,[1] and Changyuan Yu[2]

[1] *Photonics Research Center, Department of Electrical Engineering, The Hong Kong Polytechnic University, Hung Hom, Kowloon, Hong Kong*
[2]*Department of Electrical and Computer Engineering, National University of Singapore, Singapore*
**shunrongshen637@gmail.com*

Abstract: Digital signal processing (DSP)-based coherent communications have become standard for future high-speed optical networks. Implementing DSP-based advanced algorithms for data detection requires much more detailed knowledge of the transmission link parameters, resulting in optical performance monitoring (OPM) being even more important for next generation systems. At the same time, the DSP platform also enables new strategies for OPM. In this paper, we propose the use of pilot symbols with alternating power levels and study the statistics of the received power and phase difference to simultaneously and independently monitor the carrier frequency offset between transmitter and receiver laser, laser linewidth, number of spans, fiber nonlinearity parameters as well as optical signal-to-noise ratio (OSNR) of a transmission link. Analytical predictions are verified by simulation results for systems with full chromatic dispersion (CD) compensation per span and 10% CD under-compensation per span. In addition, we show that by monitoring the changes in the statistics of the received pilot symbols during network operation, one can locate faults or OSNR degradations along a transmission link without additional monitoring equipments at intermediate nodes, which may be useful for more efficient dynamic routing and network management.

OCIS codes: (060.0060) Fiber optics and optical communications; (060.1660) Coherent communications; (060.4370) Nonlinear optics, fibers.

References and links

1. Z. Q. Pan, C. Y. Yu, and A. E. Willner, "Optical performance monitoring for the next generation optical communication networks," Opt. Fiber Technol. **16**(1), 20–45 (2010).
2. S. Zhang, *et al*., "Novel ultra wide-range frequency offset estimation for digital coherent optical receiver," in Optical Fiber Communication/National Fiber Optic Engineers Conference, (OFC/NFOEC), 2010, Paper OWV3.
3. Y. Cao, S. Yu, J. Shen, W. Gu, and Y. Ji, "Frequency Estimation for Optical Coherent MPSK System Without Removing Modulated Data Phase," IEEE Photon. Technol. Lett. **22**(10), 691–693 (2010).
4. T. Duthel, G. Clarici, C. R. S. Fludger, J. C. Geyer, C. Schulien, and S. Wiese, "Laser Linewidth Estimation by Means of Coherent Detection," IEEE Photon. Technol. Lett. **21**(20), 1568–1570 (2009).
5. A. P. T. Lau, and J. M. Kahn, "Signal design and detection in presence of nonlinear phase noise," J. Lightwave Technol. **25**(10), 3008–3016 (2007).
6. K. P. Ho, and J. M. Kahn, "Electronic compensation technique to mitigate nonlinear phase noise," J. Lightwave Technol. **22**(3), 779–783 (2004).
7. A. P. T. Lau, S. Rabbani, and J. M. Kahn, "On the Statistics of Intrachannel Four-Wave Mixing in Phase-Modulated Optical Communication Systems," J. Lightwave Technol. **26**(14), 2128–2135 (2008).
8. E. Ip, and J. M. Kahn, "Compensation of Dispersion and Nonlinear Impairments Using Digital Backpropagation," J. Lightwave Technol. **26**(20), 3416–3425 (2008).
9. E. F. Mateo, and G. F. Li, "Compensation of interchannel nonlinearities using enhanced coupled equations for digital backward propagation," Appl. Opt. **48**(25), F6–F10 (2009).
10. K. S. Kim, R. H. Stolen, W. A. Reed, and K. W. Quoi, "Measurement of the nonlinear index of silica-core and dispersion-shifted fibers," Opt. Lett. **19**(4), 257–259 (1994).

#135675 - $15.00 USD Received 27 Sep 2010; revised 21 Oct 2010; accepted 21 Oct 2010; published 26 Oct 2010

11. T. Kato, Y. Suetsugu, M. Takagi, E. Sasaoka, and M. Nishimura, "Measurement of the nonlinear refractive index in optical fiber by the cross-phase-modulation method with depolarized pump light," Opt. Lett. **20**(9), 988–990 (1995).
12. L. Prigent, and J. P. Hamaide, "Measurement of Fiber Nonlinear Kerr Coefficient by four-Wave-Mixing," IEEE Photon. Technol. Lett. **5**(9), 1092–1095 (1993).
13. C. Xu, and X. Liu, "Postnonlinearity compensation with data-driven phase modulators in phase-shift keying transmission," Opt. Lett. **27**(18), 1619–1621 (2002).
14. M. N. Petersen, and M. L. Nielsen, "Experimental and theoretical demonstration of launch power optimisation using subcarrier fibre nonlinearity monitor," Electron. Lett. **41**(5), 268–269 (2005).
15. M. Mayrock, and H. Haunstein, "Monitoring of Linear and Nonlinear Signal Distortion in Coherent Optical OFDM Transmission," J. Lightwave Technol. **27**(16), 3560–3566 (2009).
16. T. Takahito, *et al*., "Semi-Blind Nonlinear Equalization in Coherent Multi-Span Transmission System with Inhomogeneous Span Parameters," in Optical Fiber Communication/National Fiber Optic Engineers Conference, (OFC/NFOEC), 2010, Paper OMR6.
17. A. P. T. Lau, and J. M. Kahn, "Design of inline amplifier gains and spacings to minimize the phase noise in optical transmission systems," J. Lightwave Technol. **24**(3), 1334–1341 (2006).
18. T. Tanimura, *et al*., "Digital clock recovery algorithm for optical coherent receivers operating independent of laser frequency offset," in 34th European Conference on Optical Communication (ECOC), (2008), Paper Mo.3.D.2.
19. Y. G. Wen, V. W. S. Chan, and L. Z. Zheng, "Efficient fault-diagnosis algorithms for all-optical WDM networks with probabilistic link failures," J. Lightwave Technol. **23**(10), 3358–3371 (2005).
20. J. H. Park, J. S. Baik, and C. H. Lee, "Fault-localization in WDM-PONs," in Optical Fiber Communication/National Fiber Optic Engineers Conference (OFC/NFOEC), 2006, Paper JThB79.
21. S. S. Ahuja, S. Ramasubramanian, and M. Krunz, "Single-Link Failure Detection in All-Optical Networks using Monitoring Cycles and Paths," IEEE/ACM Transactions on Networking, **17**, 1080–1093 (2009).
22. A. V. Sichani, and H. T. Mouftah, "Limited-perimeter vector matching fault-localization protocol for transparent all-optical communication networks," IET Communications **1**(3), 472–478 (2007).
23. M. Khair, B. Kantarci, J. Zheng, and H. T. Mouftah, "Optimization for Fault Localization in All-Optical Networks," J. Lightwave Technol. **27**(21), 4832–4840 (2009).

1. Introduction

Optical performance monitoring (OPM) has become increasingly important in recent years due to the rapid developments in dynamic optical networks with reconfigurable optical add drop multiplexers (ROADM) [1]. The need for self-diagnosed systems and real-time channel monitoring is vital to ensure robust transmission especially for next generation systems operating at 100Gb/s per channel and above. As both industries and academia are currently moving towards higher-order modulation formats using coherent detection, the impact of signal distortions caused by laser frequency offsets between the transmitter (Tx) laser and the local oscillator (LO) at the receiver (Rx) and their laser linewidths are drawing more and more attention in addition to distortions caused by chromatic dispersion (CD), polarization-mode dispersion (PMD) and optical signal-to-noise ratio (OSNR). Different techniques have been proposed for the monitoring of these two parameters such as a dual-stage frequency offset monitor (FOE) with a monitoring range up to 90% of the symbol rate in QPSK system is proposed in [2]. Cao *et al.* [3] proposed a technique for frequency offset monitoring without removing the signal phase. Furthermore, Duthel *et al.* [4] demonstrated laser linewidth monitoring by means of coherent detection with a monitoring range up to 1 MHz.

Meanwhile, contrary to older generation systems where nonlinearity is believed to be a fundamental impairment that system designers have to simply avoid, new impairment compensation techniques based on advanced DSP algorithms such as nonlinear phase noise compensation [5,6], intra-channel four-wave mixing compensation [7] and digital back-propagation (BP) [8,9] have been proposed to mitigate the effect of fiber nonlinearity-induced impairments. However, such techniques require detail knowledge of various parameters of the link including the nonlinear coefficients of fibers, number of spans N and the dispersion map (as supposed to just accumulated CD) of the link. Furthermore, as shown in Fig. 1(a), dynamic routing in practical terrestrial networks will still result in variations of link parameters such as N from time to time. To evaluate the performance impact with imperfect knowledge of the link, Fig. 1(b) shows the resulting Q-factor using BP with incorrect parameter values for a 1600 km system with 20 spans and 10% CD under-compensation per span. The modulation format is 200 Gb/s polarization-multiplexed Non Return-to-Zero (NRZ)-16-quadrature amplitude modulation (QAM) and the specifications of other link parameters are shown in

#135675 - $15.00 USD Received 27 Sep 2010; revised 21 Oct 2010; accepted 21 Oct 2010; published 26 Oct 2010

Table 1 (in Section 3). The oversampling rate is 2 and the ξ parameter of the BP algorithm described in [8] has been optimized. The *Q*-factor corresponding to algorithms that only compensate for CD is also shown as reference. From the figures, it can be seen that when the number of spans used in BP is smaller than the actual value by 3, the performance improvements by using BP is noticeably reduced. On the other hand, over-estimating *N* will be equivalent to BP with multi-span step size, which increases computational complexity [8]. Similarly, the fiber nonlinear coefficient γ needs to be monitored with good accuracy at the receiver in order to fully optimize the performance of BP. Various approaches have been proposed to measure the nonlinear coefficients of short fibers utilizing the effect of self-phase modulation (SPM) [10], cross-phase modulation (XPM) [11] and four-wave mixing (FWM) [12] with special experimental setups. Launch power optimization based on monitoring of fiber nonlinearity induced signal degradations are also studied for a given transmission link [13–15]. However, there has been no means of direct estimation of fiber nonlinear coefficients in a communication system. The value of *N* may be given by upper layer protocols from the control plane but it may not be available sometimes. To this end, Tanimura et al. [16] studied the use of semi-blind sequences for optimizing the nonlinear equalization parameters in BP given an almost perfect prior knowledge of the transmission link. However, a thorough investigation on the monitoring of fiber nonlinear coefficients and number of spans are much needed for practical implementations of advanced DSP algorithms like BP in a dynamic network environment.

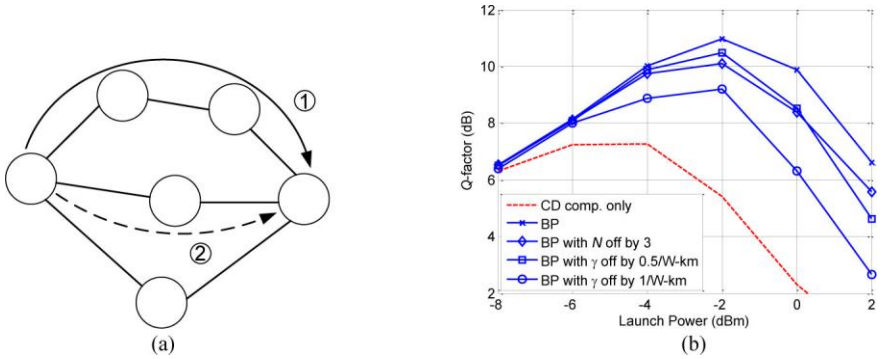

Fig. 1. (a) In a dynamic optical network with ROADMs, signal may travel through different routes even for a given source and destination. This results in variations of the number of spans *N* as well as other parameters of the overall transmission link. (b) *Q*-factor vs. launch power for a NRZ-16-QAM system with length 1600 km and 10% CD under-compensation per span. System performance is sensitive to the accuracies of the parameters used in BP.

In this paper, we propose the use of pilot symbols with alternating power levels and study their statistics such as the means and variances of received signal power and phase difference to jointly and independently monitor frequency offsets, laser linewidths, number of spans, fiber nonlinear coefficients as well as OSNR of the link. Analytical predictions are verified through simulation results for links with dispersion maps commonly used in practice. As the phase difference rather than the absolute phase of the received pilot symbols are monitored, the proposed technique should be robust against other phase-perturbing mechanisms that are slower than the sampling rate of the DSP. Finally, for a given link, we will show that by monitoring the changes in the variances of the received power and phase difference from time to time, one can locate faults or identify specific points in a transmission link with a sudden decrease in OSNR. Such fault localization technique has the advantage that no monitoring equipment is needed at intermediate nodes of the link.

#135675 - $15.00 USD Received 27 Sep 2010; revised 21 Oct 2010; accepted 21 Oct 2010; published 26 Oct 2010

2. Simultaneous and independent multi-parameters monitoring using pilot symbols

2.1. System model

Consider a coherent optical communication system consisting of *N* spans of single-mode fiber (SMF) with length L_S followed by a dispersion compensating module with 2-stage amplifiers and dispersion compensation fibers (DCF) of length L_D as shown in Fig. 2. The gain of amplifiers exactly compensates for the fiber loss in the previous span. The received signal is coherently mixed with optical wave generated by local oscillator (LO) and passes through balanced detectors where the in-phase and quadrature outputs are sampled and processed in a DSP unit. To monitor various channel parameters, a sequence of pilot symbols with period *T* and alternating power levels P_1 and P_2 as shown in Fig. 3 is sent into the link prior to data transmission. The symbol rate 1/*T* will be chosen such that inter-symbol interference (ISI) and pulse shape distortion induced by chromatic dispersion (CD) and polarization-mode dispersion (PMD) is negligible. In addition, as the symbol rate of pilot sequence is much lower than that of data transmission, pulse distortion caused by filters designed for 25 GSym/s transmission and beyond should be negligible as well. Let $n_{S_i}(t)$ and $n_{D_i}(t)$ be the amplified spontaneous emission (ASE) noise from optical amplifiers following the SMF and DCF of the i^{th} span respectively which are zero-mean complex circularly symmetric Gaussian random processes with power spectral density

$$S_{S(D)}(f) = n_{sp} h\nu \left(e^{\alpha_{S(D)} L_{S(D)}} - 1 \right)$$

where n_{sp} is the spontaneous emission factor, ν is the carrier frequency, $\alpha_{S(D)}$ is the attenuation coefficient of the SMF (DCF) and *h* is the Planck constant.

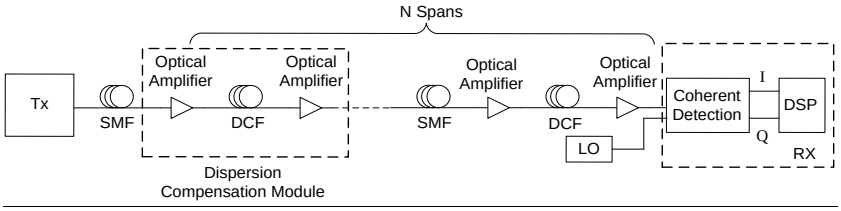

Fig. 2. A coherent communication system setup with optical CD compensation

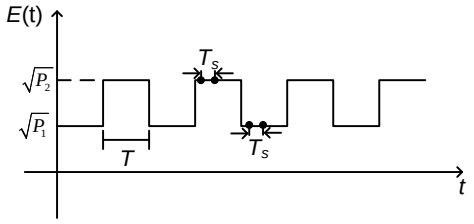

Fig. 3. A sequence of pilot symbols with alternating power levels P_1 and P_2 for the monitoring of laser linewidth, frequency offset, number of spans, fiber nonlinear parameters and OSNR of the link. The received signal is sampled at a rate of $1/T_s$ and the symbol rate 1/*T* is low enough such that the transmitted signal *E(t)* does not undergo any pulse shape distortion due to CD and/or PMD.

In absence of nonlinearity and when the symbol rate of the pilot symbols is low enough so that the effects of CD and PMD are negligible, the instantaneous received signal power at time *t* can be expressed as

#135675 - $15.00 USD Received 27 Sep 2010; revised 21 Oct 2010; accepted 21 Oct 2010; published 26 Oct 2010

$$P(t)=\left|\sqrt{P_k}+\sum_{i=1}^{N}\left(n_{S_i}(t)+n_{D_i}(t)\right)\right|^2 \approx P_k+2\sqrt{P_k}\,\mathrm{Re}\left\{\sum_{i=1}^{N}\left(n_{S_i}(t)+n_{D_i}(t)\right)\right\} \qquad \text{for } k=1,2 \qquad (1)$$

where the approximation is valid for high OSNR. The variance of the received signal power P_k is then given by

$$\begin{aligned}\sigma^2_{power}(P_k) &= \mathbf{E}\left[P^2(t)\right]-\mathbf{E}\left[P(t)\right]^2 \\ &= \mathbf{E}\left[P_k^2+4P_k\sqrt{P_k}\,\mathrm{Re}\left\{\sum_{i=1}^{N}\left(n_{S_i}(t)+n_{D_i}(t)\right)\right\}+4P_k\left(\sum_{i=1}^{N}\mathrm{Re}\left\{n_{S_i}(t)+n_{D_i}(t)\right\}\right)^2\right]-P_k^2 \\ &= 2P_kN\left(\sigma_S^2+\sigma_D^2\right) \qquad \text{for } k=1,2.\end{aligned}$$

(2)

where $\sigma^2_{S(D)}=S_{S(D)}(f)B_f$ and B_f is the low-pass filter bandwidth at the receiver. It should be noted that Eq. (2) is still valid for systems with fiber nonlinearity.

The overall received phase $\phi(t)$ after propagating through *N* spans of fibers is given by

$$\phi(t)=\phi_{ASE}(t)+\phi_{NL}(t)+\phi_{Tx}(t)+\phi_{Rx}(t)+2\pi\Delta f_{off}t+\theta \qquad (3)$$

which contains ASE-induced phase noise $\phi_{ASE}(t)$, nonlinear phase noise $\phi_{NL}(t)$ caused by fiber nonlinearity as well as transmitter and receiver laser phase noise $\phi_{Tx}(t)$ and $\phi_{Rx}(t)$. The frequency offset between the transmitter and receiver phase noise is denoted by Δf_{off} and θ is the relative phase of the transmitter (Tx) and receiver (Rx) laser at *t* = 0. For high OSNR, the ASE-induced phase noise can be approximated as

$$\phi_{ASE}(t)\approx\frac{\mathrm{Im}\left\{\sum_{i=1}^{N}\left[n_{S_i}(t)+n_{D_i}(t)\right]\right\}}{\sqrt{P_k}} \qquad \text{for } k=1,2 \qquad (4)$$

with zero mean and variance

$$\sigma^2_{ASE}(P_k)=\frac{N}{2P_k}\left(\sigma_S^2+\sigma_D^2\right) \qquad \text{for } k=1,2. \qquad (5)$$

Let γ_S and γ_D be the nonlinear coefficients of the SMF and DCF, and $L_{eff,S}$ and $L_{eff,D}$ be the effective lengths of SMF and DCF respectively. Defining $\Lambda_S=\gamma_S L_{eff,S}$ and $\Lambda_D=\gamma_D L_{eff,D}$, the overall nonlinear phase shift at the receiver is given by

#135675 - $15.00 USD Received 27 Sep 2010; revised 21 Oct 2010; accepted 21 Oct 2010; published 26 Oct 2010

$$
\begin{aligned}
\phi_{NL}(t) &= \Lambda_S \left|\sqrt{P_k}\right|^2 + \Lambda_D \left|\sqrt{P_k} + n_{S_1}(t)\right|^2 \\
&\quad + \Lambda_S \left|\sqrt{P_k} + n_{S_1}(t) + n_{D_1}(t)\right|^2 + \Lambda_D \left|\sqrt{P_k} + n_{S_1}(t) + n_{D_1}(t) + n_{S_2}(t)\right|^2 + \cdots \\
&\quad + \Lambda_S \left|\sqrt{P_k} + n_{S_1}(t) + \cdots n_{S_{N-1}}(t) + n_{D_1}(t) + \cdots + n_{D_{N-1}}(t)\right|^2 \\
&\quad + \Lambda_D \left|\sqrt{P_k} + n_{S_1}(t) + \cdots\cdots n_{S_N}(t) + n_{D_1}(t) + \cdots\cdots + n_{D_{N-1}}(t)\right|^2 \qquad (6) \\
&= \sum_{i=1}^{N} \left(\Lambda_D \left|\sqrt{P_k} + \sum_{l=1}^{i} n_{S_l}(t) + \sum_{m=1}^{i-1} n_{D_m}(t)\right|^2 + \Lambda_S \left|\sqrt{P_k} + \sum_{m=1}^{i-1} n_{S_m}(t) + \sum_{m=1}^{i-1} n_{D_m}(t)\right|^2 \right) \\
&\approx \sum_{i=1}^{N} \Lambda_D \left(P_k + 2\sqrt{P_k}\,\mathrm{Re}\left\{ \sum_{l=1}^{i} n_{S_l}(t) + \sum_{m=1}^{i-1} n_{D_m}(t) \right\} \right) \\
&\quad + \sum_{i=1}^{N} \Lambda_S \left(P_k + 2\sqrt{P_k}\,\mathrm{Re}\left\{ \sum_{l=1}^{i-1} n_{S_l}(t) + \sum_{m=1}^{i-1} n_{D_m}(t) \right\} \right) \qquad \text{for } k = 1, 2.
\end{aligned}
$$

where the approximation is valid for high OSNR. In this case, the mean and variance of the nonlinear phase shift $\phi_{NL}(t)$ is given by

$$
\overline{\phi_{NL}(P_k)} = P_k N (\Lambda_S + \Lambda_D) \qquad \text{for } k = 1, 2 \qquad (7)
$$

and

$$
\begin{aligned}
\sigma_{NL}^2(P_k) &= \mathrm{E}\left[\phi_{NL}^2(P_k)\right] - \mathrm{E}\left[\phi_{NL}(P_k)\right]^2 \\
&= 2P_k (\Lambda_S + \Lambda_D)^2 \sigma_D^2 \left[(N-1)^2 + (N-2)^2 + \cdots + 1 \right] \\
&\quad + 2P_k \sigma_S^2 \left\{ \left[\Lambda_S (N-1) + \Lambda_D N \right]^2 + \left[\Lambda_S (N-2) + \Lambda_D (N-1) \right]^2 + \cdots + \Lambda_D^2 \right\} \\
&= 2P_k (\Lambda_S + \Lambda_D)^2 \sigma_D^2 \sum_{i=1}^{N-1} i^2 + 2P_k \sigma_S^2 \left(\Lambda_S^2 \sum_{i=1}^{N-1} i^2 + \Lambda_D^2 \sum_{i=1}^{N} i^2 \right) \\
&\quad + 4\Lambda_S \Lambda_D P_k \sigma_S^2 \sum_{i=0}^{N-1} (N-i)^2 - 4\Lambda_S \Lambda_D P_k \sigma_S^2 \sum_{i=0}^{N-1} (N-i) \qquad \text{for } k = 1, 2.
\end{aligned}
$$

As $\sum_{i=1}^{N} i^2 = \dfrac{N(N+1)(2N+1)}{6}$ and $\sum_{i=1}^{N} i = \dfrac{N(N+1)}{2}$,

$$
\begin{aligned}
\sigma_{NL}^2(P_k) &= 2P_k (\Lambda_S + \Lambda_D)^2 \sigma_D^2 \frac{N(N-1)(2N-1)}{6} \qquad (8) \\
&\quad + 2P_k \sigma_S^2 \left[\Lambda_S^2 \frac{N(N-1)(2N-1)}{6} + \Lambda_D^2 \frac{N(N+1)(2N+1)}{6} \right] \\
&\quad + 4\Lambda_S \Lambda_D P_k \sigma_S^2 \left[\frac{N(N+1)(2N+1)}{6} - \frac{N(N+1)}{2} \right] \\
&= 2P_k (\Lambda_S + \Lambda_D)^2 (\sigma_S^2 + \sigma_D^2) \left(\frac{1}{3} N^3 - \frac{1}{2} N^2 + \frac{1}{6} N \right) \\
&\quad + 2P_k \sigma_S^2 \left[\Lambda_D^2 N^2 + \Lambda_S \Lambda_D (N^2 - N) \right] \qquad \text{for } k = 1, 2.
\end{aligned}
$$

#135675 - $15.00 USD Received 27 Sep 2010; revised 21 Oct 2010; accepted 21 Oct 2010; published 26 Oct 2010

Assuming Tx and Rx lasers with identical linewidth, the spectrum of the laser output $e^{j\phi_{Tx(Rx)}(t)}$ can be modeled as a Lorentzian lineshape with 3-dB linewidth Δf_{LW} in which

$$\mathbf{E}\left[e^{j(\phi_{Tx(Rx)}(t_1)-\phi_{Tx(Rx)}(t_2))} \right] = \exp(-\pi\Delta f_{LW}|t_1-t_2|). \tag{9}$$

Equivalently, the phase noise $\phi_{Tx(Rx)}(t)$ can be modeled as a Wiener process in which $\phi_{Tx(Rx)}(t_2)-\phi_{Tx(Rx)}(t_1)$ is Gaussian distributed with zero mean and variance

$$\sigma_{LW}^2 = 2\pi\Delta f_{LW}|t_1-t_2|. \tag{10}$$

In the following section, we will derive equations to monitor the frequency offset, laser linewidth, number of spans *N*, OSNR as well as the nonlinear coefficients of the link from the statistics of the received power and phase difference. It should be noted that for the purpose of implementing advanced DSP algorithms like BP, it suffices to monitor the nonlinear parameter Λ_D as supposed to the fiber nonlinear coefficient γ_D.

2.2. Simultaneous and independent multi-parameter monitoring

The frequency offset between the Tx and Rx lasers and their linewidths can be obtained from the statistics of the phase difference between samples within a pilot symbol. Without loss of generality, let $\phi(t)$ and $\phi(t+w_1T_s)$ belong to the same pilot symbol with power $\sqrt{P_k}$ and $\phi(t)$ being the first sample of the symbol. The phase difference between these two samples is given by

$$\begin{aligned}\Delta\phi(w_1) &= \phi(t+w_1T_s)-\phi(t)\\ &= \left[\phi_{ASE}(t)+\phi_{NL}(t)+\phi_{Tx}(t)+\phi_{Rx}(t)\right]-\\ &\quad \left[\phi_{ASE}(t+w_1T_s)+\phi_{NL}(t+w_1T_s)+\phi_{Ix}(t+w_1T_s)+\phi_{Rx}(t+w_1T_s)\right]+2\pi\Delta f_{off}w_1T_s\end{aligned}$$

where $w_1 = 1,2,\cdots\eta-1$ and $\eta = T/T_s$ is the number of samples per symbol. As $\phi_{ASE}(t)$ and $\phi_{NL}(t)$ are uncorrelated with each other [17] and $\phi_{ASE(NL)}(t)$ and $\phi_{ASE(NL)}(t+w_1T_s)$ are also uncorrelated if we choose the filter bandwidth $B_f = \frac{1}{2T_s}$, the mean and variance of $\Delta\phi(w_1)$ is given by

$$\overline{\Delta\phi(w_1)} = 2\pi\Delta f_{off}w_1T_s \tag{11}$$

and

$$\sigma_{\Delta\phi,k}^2(w_1) = 2\sigma_{NL}^2(P_k)+2\sigma_{ASE}^2(P_k)+2\times2\pi\Delta f_{LW}w_1T_s \tag{12}$$

It is obvious from Eq. (12) that the linear and nonlinear phase noise variance $\sigma_{ASE}^2(P_k)$ and $\sigma_{NL}^2(P_k)$ do not depend on w_1. Therefore, for two values w_1 and w_2 such that $\phi(t)$, $\phi(t+w_1T_s)$ and $\phi(t+w_2T_s)$ belong to the same pilot symbol, the difference between $\sigma_{\Delta\phi,k}^2(w_1)$ and $\sigma_{\Delta\phi,k}^2(w_2)$ can be expressed as

$$\sigma_{\Delta\phi,k}^2(w_1)-\sigma_{\Delta\phi,k}^2(w_2) = 2\times2\pi\Delta f_{LW}(w_1-w_2)T_s \tag{13}$$

With (11) and (13), the frequency offset and laser linewidth of the Tx and Rx lasers can be estimated by

#135675 - $15.00 USD Received 27 Sep 2010; revised 21 Oct 2010; accepted 21 Oct 2010; published 26 Oct 2010

$$\Delta f_{off} = \frac{\overline{\Delta\phi}(w_1)}{2\pi w_1 T_s} \tag{14}$$

and

$$\Delta f_{LW} = \frac{\sigma^2_{\Delta\phi,k}(w_2) - \sigma^2_{\Delta\phi,k}(w_1)}{4\pi(w_2 - w_1)T_s} \tag{15}$$

The statistics of the phase difference $\Delta\phi(w_1)$ also allow us to simultaneously and independently monitor the number of spans *N*, fiber nonlinear parameters as well as OSNR of the link. In particular, if we choose $w_1 = \eta$, the two samples $\phi(t)$ and $\phi(t + w_1 T_s)$ will belong to different pilot symbols with different power levels. In this case, the mean of the phase difference will be given by

$$\overline{\Delta\phi(\eta)} = (P_2 - P_1)N(\Lambda_S + \Lambda_D) + 2\pi\Delta f_{off} T \tag{16}$$

assuming the signal power at time *t* is $P(t) = P_1$.

As the parameters of SMF such as length, attenuation and nonlinear coefficients are usually known and relatively more consistent across a network compared to those of DCF in practice, we will assume the knowledge of σ_S^2 and Λ_S when monitoring the number of span *N*, fiber nonlinear coefficient and OSNR of the link. With Eqs. (2), (5), (8), (12)-(16) and some algebraic manipulations, one obtain

$$\begin{aligned} 2(P_1+P_2)\sigma_S^2\left(\Lambda_S^2 - \Lambda_S\frac{\overline{\Delta\phi(\eta)}}{P_1-P_2}\right)N^3 + \Bigg[(P_1+P_2)\frac{\overline{\Delta\phi(\eta)}^2\sigma^2_{power}(P_1)}{3(P_1-P_2)^2P_1} + 2(P_1+P_2)\sigma_S^2\frac{\overline{\Delta\phi(\eta)}^2}{(P_1-P_2)^2} \\ -2(P_1+P_2)\Lambda_S\sigma_S^2\frac{\overline{\Delta\phi(\eta)}}{P_1-P} + \frac{\sigma^2_{power}(P_1)}{4P_1}\left(\frac{1}{P_1}+\frac{1}{P_2}\right) - \left(\sigma^2_{\Delta\phi,1}(w_1) + \sigma^2_{\Delta\phi,2}(w_2)\right)\Bigg]N^2 \\ -\frac{(P_1+P_2)\overline{\Delta\phi(\eta)}^2\sigma^2_{power}(P_1)}{2P_1(P_1-P_2)^2}N + \frac{(P_1+P_2)\overline{\Delta\phi(\eta)}^2\sigma^2_{power}(P_1)}{6P_1(P_1-P_2)^2} = 0 \end{aligned} \tag{17}$$

which is a cubic function of *N*. Subsequently, the fiber nonlinear parameter Λ_D and OSNR can be calculated by

$$\Lambda_D = \frac{\overline{\Delta\phi(\eta)} - 2\pi\Delta f_{off} T}{(P_1 - P_2)N} - \Lambda_S \tag{18}$$

and

$$\text{OSNR} = \frac{P_k}{N(\sigma_S^2 + \sigma_D^2)} = \frac{P_k}{\frac{\sigma^2_{power}}{2P_k}} = \frac{2P_k^2}{\sigma^2_{power}} \qquad \text{for } k = 1, 2. \tag{19}$$

In summary, we can estimate frequency offset, laser linewidth, number of spans, fiber nonlinear parameter and OSNR of a transmission llink by choosing arbitrary values of P_1, P_2, w_1 and w_2 and solving for Eqs. (14), (15), (17), (18) and (19).

#135675 - $15.00 USD Received 27 Sep 2010; revised 21 Oct 2010; accepted 21 Oct 2010; published 26 Oct 2010

3. Simulation Results and Discussions

Simulations are conducted to investigate the monitoring performance of Δf_{off} , Δf_{LW} ,N, Λ_D and OSNR. Pilot sequences with 10^6 symbols with NRZ pulse shape are transmitted at two arbitrarily chosen power levels of $P_1 = -3$ dBm and $P_2 = -2$ dBm. The symbol rate is chosen to be 50 MSym/s so that the effects of CD and PMD become negligible. The sampling rate is set to be 25 GHz and thus $\eta = 500$. In our simulations, high analog-to-digital converter resolution (ADC) and timing recovery are assumed and other channel parameters are listed in Table 1. To maximize the monitoring range of Δf_{off} for a given sampling rate, w_1 is chosen to be 1. In addition, we arbitrarily set $w_2 = 3$ for laser linewidth monitoring. Simulation results for frequency offset and laser linewidth monitoring for a 15-span system are shown in Figs. 4(a) and 4(b) for full CD compensated and 10% CD under-compensated links. The means and standard deviations of the estimates are obtained from 10 independent trials with independent ASE noise. From the figures, the proposed technique enables a wide monitoring range from −10 GHz to 10GHz, more than sufficient for worst cases of ± 5 GHz reported in practical systems [18]. The corresponding maximum estimation error is below 6 MHz. For laser linewidth monitoring, a wide dynamic range of 100 kHz to 10 MHz with corresponding maximum estimation error below 1% is achieved. Such monitoring performance is comparable to others reported in the literature [4] that only monitors laser linewidths. It is also noted that the monitoring performance does not depend on the dispersion map of the transmission link.

Table 1. Channel parameters used in simulations

Parameter	Value	Parameter	Value
α_S	0.25 dB/km	α_D	0.6 dB/km
L_S	80 km	L_D	16 km for full CD compensation 14.4 km for 10% CD under-compensation
D_S	17 ps/km·nm	D_D	−85 ps/km·nm
n_{sp}	2	ν	193.1 THz
γ_S	1.2 W^{-1}/km		

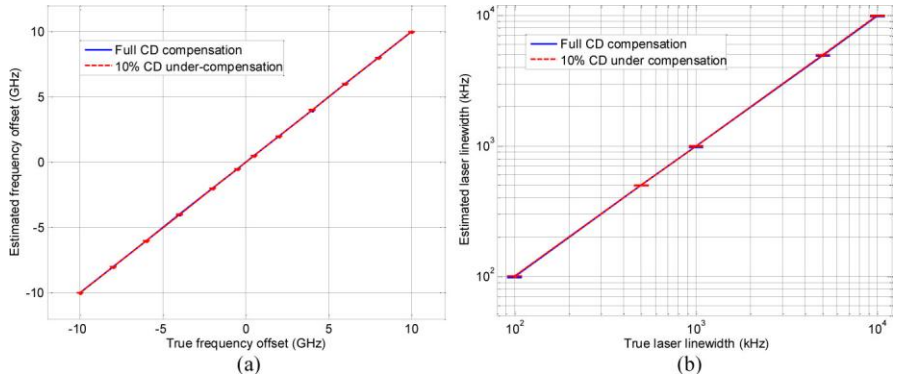

Fig. 4. (a) Estimated frequency offset vs. true frequency offset (b) Estimated laser linewidth vs. true laser linewidth for a 15-span system. Samples from 10^6 symbols are used for each estimate and the error bars indicate standard deviations of 10 independent estimates.

To ensure the monitoring accuracy of N, Λ_D and OSNR, the samples are further low-pass filtered with a bandwidth of 800 MHz and correspondingly down-sampled to eliminate the effect of CD on ASE noise. Figure 5 shows the estimated N, OSNR and Λ_D vs. their true

#135675 - $15.00 USD Received 27 Sep 2010; revised 21 Oct 2010; accepted 21 Oct 2010; published 26 Oct 2010

values for full CD compensated and 10% CD under-compensated links. The frequency offset and the laser linewidths are 200 MHz and 100 kHz respectively. As shown in Fig. 5(a), the mean of the estimated N generally agrees with their true values for $N \leq 22$. The slight inaccuracies for $N > 22$ may be caused by accumulated CD, frequency offset, laser linewidth, or a combination of them. Although the estimation errors gradually increase with N, the errors are limited to 1 span for a system containing around 25 spans. The OSNR monitoring accuracies shown in Fig. 5(b) for both dispersion maps with fiber nonlinearity are within 0.1 dB. The OSNR monitoring results are independent of the two dispersion maps and intra-channel nonlinearities. Figure 5(c) shows the estimated Λ_D for different values of Λ_D for a system with $N = 15$. Although estimation errors can be observed for both dispersion maps, the errors are limited to 0.4 dB and 0.6 dB (or equivalently 0.51 and 0.78 W^{-1}/km in γ_D) for full CD compensated and 10% CD under-compensated links respectively. In addition, it can also be shown that estimation remain fairly accurate when a few of spans have lengths slightly different than the rest of the link or when the knowledge of σ_S^2 and Λ_S is around 10% off from their true values.

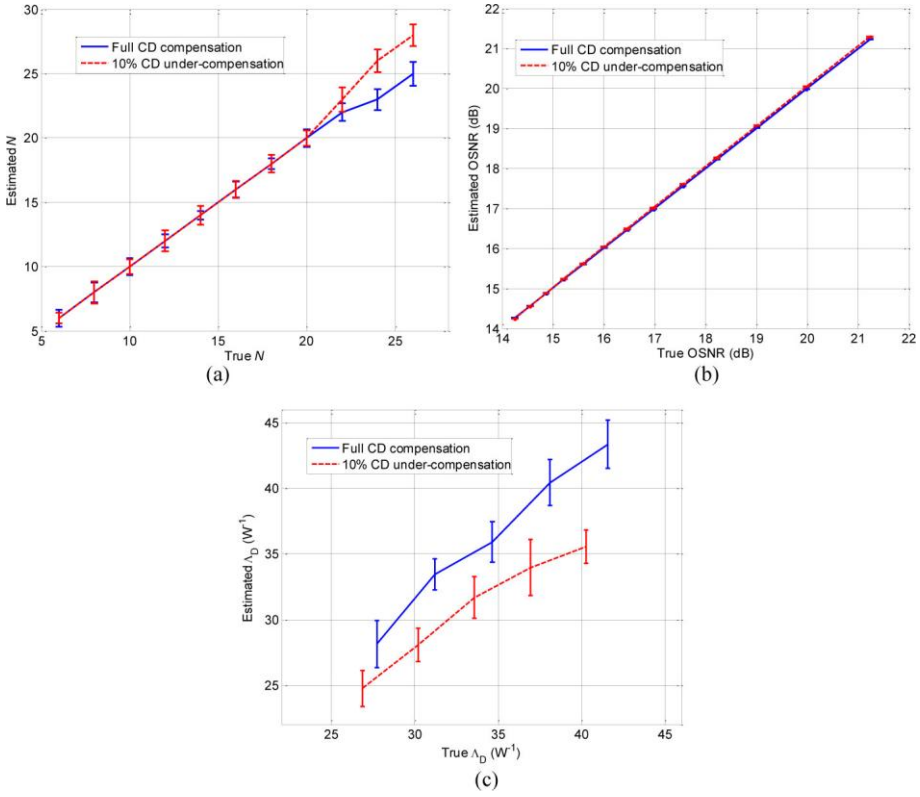

Fig. 5. (a) Estimated N vs. true N. (b) Estimated OSNR vs. true OSNR. (c) Estimated Λ_D vs. true Λ_D. Samples from 10^6 symbols are used for each estimate and the error bars indicate standard deviations of 10 independent estimates. The frequency offset and laser linewidth are 200 MHz and 100 kHz respectively.

4. Receiver-based fault localization using statistics of received pilot symbols

Data communications in optical networks can be interrupted by different types of faults along the link such as fiber cut, fiber bend and/or malfunctioning of inline optical amplifiers that result in sudden OSNR degradation or complete failure of the link. Locating the position of

#135675 - $15.00 USD Received 27 Sep 2010; revised 21 Oct 2010; accepted 21 Oct 2010; published 26 Oct 2010

such faults is crucial to network operators for efficient channel restoration and maintaining high quality of service (QoS) in dynamic network environments. When there is an undesired drop in signal power, the extra gain required to amplify the signal back to pre-determined levels will produce additional ASE noise which result in OSNR degradations at the receiver [19]. To locate faults, tunable optical time-domain reflectometer (OTDR) is proposed in [20] for the localization of fiber cut and serious degradation in OSNR. In [21], an optical transceiver is assigned to each predefined monitoring cycles to setup a dedicated supervisory channel. However, introduction of additional optoelectronic components will increase the cost of installation and maintenance, especially in large scale networks. Meanwhile, Sichani *et al.* [22] demonstrated the use of limited-perimeter vector matching fault-localization protocol to achieve efficient fault localization in large scale networks by analyzing the alarm message issued by multiple devices. One disadvantage of this approach is that at least two distinct lightpaths with separate source-destination pairs are required [23].

If we regularly insert the pilot symbols studied in this paper between data transmission, it is actually possible to locate faults without the need of monitoring equipments at intermediate points of the link by studying the changes in the statistics of the received signal power and phase difference. In particular from Eqs. (2) and (8), if sudden OSNR degradations occur at the i^{th} span, the increase in the ASE noise power of the i^{th} amplifier $\Delta\sigma_i^2$ will induce the same change in the received power variance $\Delta\sigma_{power}^2(P_k)$ regardless of the value of i. However, the induced change in the variance of phase difference $\Delta\sigma_{\Delta\phi,k}^2(1)$ will actually depend on i. Intuitively, this is because ASE noise introduced earlier in the transmission link undergoes more fiber nonlinear effects and accumulates more nonlinear phase noise. Therefore, by monitoring $\Delta\sigma_{power}^2(P_k)$ and $\Delta\sigma_{\Delta\phi,k}^2(1)$ due to sudden OSNR degradations, one can determine the amount and location of the additional ASE noise introduced in the link which in term serves as an indication of the location of the fault.

A calibration graph of the fault locations indexed according to the number of span starting from the transmitter vs. $\Delta\sigma_{\Delta\phi,k}^2(1)$ for different $\Delta\sigma_i^2$ is given in Fig. 6 for a 20-span link. The other parameters of the pilot sequence and the channel used in the simulation are identical to those in Section 3. From the figure, for a given $\Delta\sigma_i^2$, the change in variance of phase difference $\Delta\sigma_{\Delta\phi,k}^2(1)$ is distinct for different fault locations. In a network where fault locations are detected through other means, the proposed method may provide additional information about the status of the network and simplify network layer communication protocols and enhance efficiencies in network management.

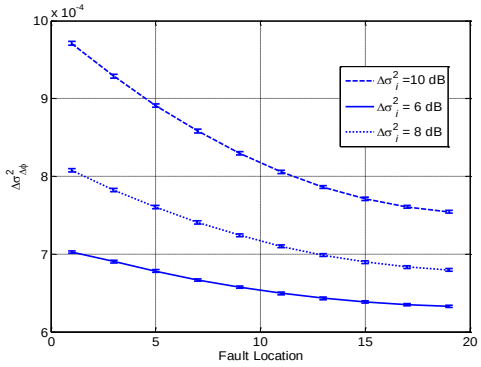

Fig. 6. Change in variance of phase difference $\Delta\sigma_{\Delta\phi}^2(1)$ vs. fault location with $\Delta\sigma_i^2 =$, 8 and 10 dB for a 20-span link. Samples from 10^6 symbols are used for each estimate and the error bars indicate standard deviations of 10 independent estimates.

#135675 - $15.00 USD Received 27 Sep 2010; revised 21 Oct 2010; accepted 21 Oct 2010; published 26 Oct 2010

5. Conclusions

In this paper, we demonstrated that DSP-based coherent communication systems require detail and accurate knowledge of transmission link parameters for appropriate and practical implementation of advanced impairment compensation algorithms such as digital back-propagation. We then proposed the use of pilot symbols prior to data transmission and study the statistics of the received power and phase difference to monitor laser frequency offset, laser linewidth, the number of spans, the fiber nonlinear parameters as well as the OSNR of the link. For links with full CD compensation or 10% CD under-compensation per span, simulation results indicated that simultaneous and independent monitoring of multiple parameters can be achieved with good monitoring range and accuracies. In addition, examining the changes in the statistics of received power and phase difference enable us to locate faults along a given transmission link without the need for monitoring equipments at intermediate nodes of the link. Experimental verifications of the proposed monitoring technique, impact of inhomogeneous fiber configuration, multi-parameter monitoring for CD-uncompensated links and the effect of WDM will be investigated in future.

Acknowledgments

The authors would like to acknowledge the support of the Hong Kong Government General Research Fund under project number 519910.

#135675 - $15.00 USD Received 27 Sep 2010; revised 21 Oct 2010; accepted 21 Oct 2010; published 26 Oct 2010